

DTNSRDC - 81 / 054

JUN 1981

DAVID W. TAYLOR NAVAL SHIP RESEARCH AND DEVELOPMENT CENTER

Bethesda, Maryland 20084



PERIODIC SINGLE-BLADE LOADS ON PROPELLERS IN TANGENTIAL AND LONGITUDINAL WAKES



by

Robert J. Boswell
Stuart D. Jessup
Ki-Han Kim

APPROVED FOR PUBLIC RELEASE: DISTRIBUTION UNLIMITED

Presented at the
PROPELLERS '81 SYMPOSIUM
The Society of Naval Architects and Marine Engineers
Virginia Beach, Virginia, May 26-27, 1981

SHIP PERFORMANCE DEPARTMENT RESEARCH AND DEVELOPMENT REPORT

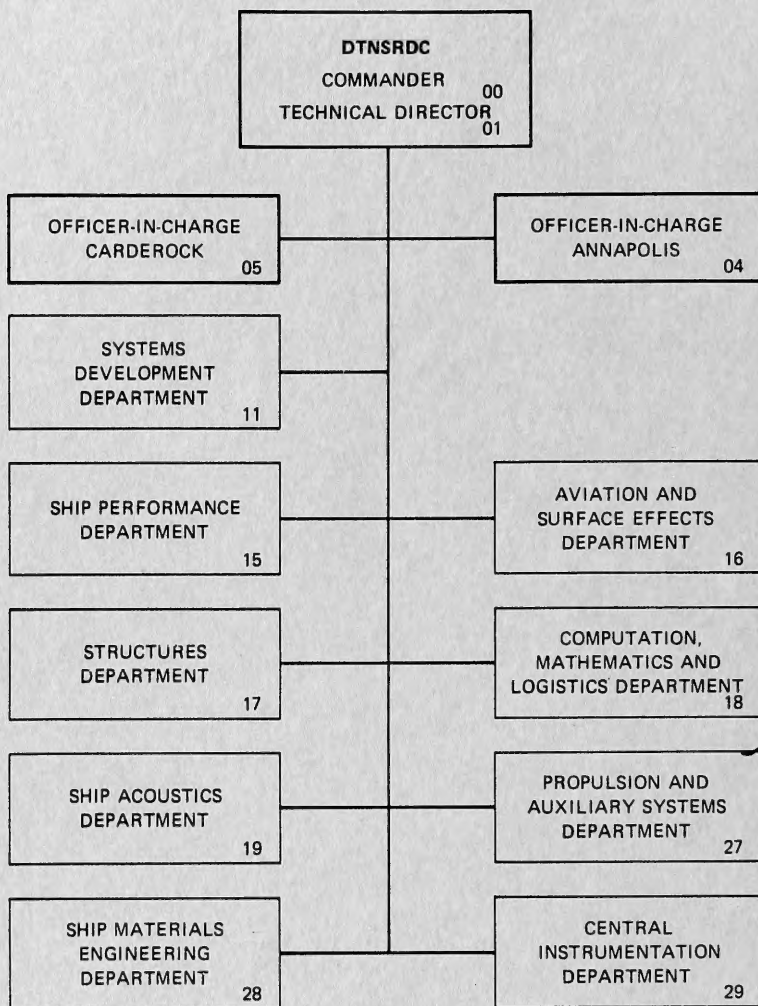
SINGLE-BLADE LOADS ON PROPELLERS IN TANGENTIAL
LONGITUDINAL WAKES

GC
1
D3
no. 81/054

June 1981

DTNSRDC-81/054

MAJOR DTNSRDC ORGANIZATIONAL COMPONENTS



UNCLASSIFIED

SECURITY CLASSIFICATION OF THIS PAGE (When Data Entered)

REPORT DOCUMENTATION PAGE		READ INSTRUCTIONS BEFORE COMPLETING FORM
1. REPORT NUMBER DTNSRDC-81/054	2. GOVT ACCESSION NO.	3. RECIPIENT'S CATALOG NUMBER
4. TITLE (and Subtitle) PERIODIC SINGLE-BLADE LOADS ON PROPELLERS IN TANGENTIAL AND LONGITUDINAL WAKES		5. TYPE OF REPORT & PERIOD COVERED Ship Performance Dept. Research and Development
		6. PERFORMING ORG. REPORT NUMBER
7. AUTHOR(s) Robert J. Boswell Stuart D. Jessup Ki-Han Kim		8. CONTRACT OR GRANT NUMBER(s)
9. PERFORMING ORGANIZATION NAME AND ADDRESS David W. Taylor Naval Ship Research and Development Center Bethesda, Maryland 20084		10. PROGRAM ELEMENT, PROJECT, TASK AREA & WORK UNIT NUMBERS (See reverse side)
11. CONTROLLING OFFICE NAME AND ADDRESS Naval Sea Systems Command (05R) Ship Systems Research and Technology Group Washington, D.C. 20362		12. REPORT DATE June 1981
14. MONITORING AGENCY NAME & ADDRESS (if different from Controlling Office) Naval Sea Systems Command (524) Propulsion Line Shafting Equipment Division Washington, D.C. 20362		13. NUMBER OF PAGES 33
16. DISTRIBUTION STATEMENT (of this Report)		15. SECURITY CLASS. (of this report) UNCLASSIFIED
		15a. DECLASSIFICATION/DOWNGRADING SCHEDULE
17. DISTRIBUTION STATEMENT (of the abstract entered in Block 20, if different from Report)		
18. SUPPLEMENTARY NOTES		
19. KEY WORDS (Continue on reverse side if necessary and identify by block number) Marine Propeller Loads Propeller Research Propulsion Model Experiments		
20. ABSTRACT (Continue on reverse side if necessary and identify by block number) Periodic single-blade loads were measured on model propellers in inclined flow and in a single-cycle circumferentially non-uniform longitudinal velocity field. The experimental results were correlated with predictions by the following methods: 1. A quasi-steady procedure developed by McCarthy at David W. Taylor Naval Ship Research and Development Center (DTNSRDC),		
(Continued on reverse side)		

UNCLASSIFIED

SECURITY CLASSIFICATION OF THIS PAGE (When Data Entered)

(Block 10)

Task Area S0379-SL001

Task 19977

Work Units 1544-296 and 1544-350

(Block 20 continued)

2. An unsteady lifting surface theory developed by Tsakonas and his colleagues at Davidson Laboratory,
3. An unsteady lifting surface theory developed by Kerwin and Lee at MIT,
4. A refinement by Kerwin to the method of Kerwin and Lee to consider the inclination of the propeller slipstream.

In inclined flow, all four of the calculation methods evaluated consistently underpredicted the experimental values of the periodic single-blade loads. The method of Kerwin, which considers the inclination of the slipstream relative to the propeller axis, produced the best correlation with experimental values. These correlations show that the inclination of the propeller slipstream relative to the propeller axis significantly influence the periodic single-blade loads. The importance of this inclination increases with increasing time-average loading.

In longitudinal flow, all of the calculation procedures predicted periodic single-blade axial force at design advance coefficient to within 20 percent of the experimental values, but agreement was not as good at off-design advance coefficients. The method of Kerwin and Lee produced the best overall correlation with experimental results considering both amplitude and phase of the periodic single-blade axial force over a range of advance coefficients.

UNCLASSIFIED

SECURITY CLASSIFICATION OF THIS PAGE (When Data Entered)

TABLE OF CONTENTS

	Page
LIST OF FIGURES	iv
LIST OF TABLES	v
ABSTRACT	1
NOMENCLATURE	1
INTRODUCTION	2
BACKGROUND	3
EXPERIMENTAL TECHNIQUES	4
WAKE SCREEN AND WAKE SURVEY	4
EXPERIMENTAL CONDITIONS AND PROCEDURES	5
DATA ACQUISITION AND ANALYSIS	6
ACCURACY	6
EXPERIMENTAL RESULTS	6
LOADING COMPONENTS	6
CENTRIFUGAL AND GRAVITATIONAL LOADS	7
VARIATION OF LOADS WITH ANGULAR POSITION	7
EFFECT OF PLATE CLEARANCE	7
EFFECT OF ADVANCE COEFFICIENT	8
CORRELATION BETWEEN EXPERIMENTAL RESULTS AND THEORETICAL PREDICTIONS	10
THEORETICAL METHODS	10
CORRELATIONS IN TANGENTIAL WAKES	11
CORRELATIONS IN LONGITUDINAL WAKES	18
SUMMARY AND CONCLUSIONS	21
ACKNOWLEDGMENTS	22
REFERENCES	22

LIST OF FIGURES

	Page
1 - Components of Blade Loading	3
2 - Sign Convention for Ship Wake Velocity Components	3
3 - Distribution of Wakes in Propeller Disks	4
4 - Experimental Variation of Loading Components with Blade Angular Position	7
5 - Effect of Plate Clearance on First Harmonic Loading in Tangential Wake	7
6 - Experimental Variation of First Harmonic Blade Loads on Propeller 4661 with Advance Coefficient	8
7 - Comparison of First Harmonic Blade Loading Coefficients in Tangential Wakes	9
8 - Comparison of Various Experimental Blade Loading Coefficients in Longitudinal Wakes	9
9 - Amplitudes of First Harmonic Blade Loads in Tangential Wakes; Correlation Between Experiment and Theory	12
10 - Phases of First Harmonic Blade Loads in Tangential Wakes; Correlation Between Experiment and Theory	14
11 - Variation of Periodic Blade Loads with Shaft Inclination	18
12 - Amplitudes of First Harmonic Blade Loads in Longitudinal Wakes; Correlation Between Experiment and Theory	19
13 - Phases of First Harmonic Blade Loads in Longitudinal Wakes; Correlation Between Experiment and Theory	19

LIST OF TABLES

	Page
1 - Characteristics of Propellers 4661, 4710, and 4402	2
2 - Comparison of Experiment and Theory in Inclined Flow - Amplitudes and Phases of First Harmonic Loading Coefficients at Design J	17
3 - Comparison of Experiment and Theory in Longitudinal Flow - Amplitudes and Phases of First Harmonic Loading Coefficients at Design J	20

ABSTRACT

Periodic single-blade loads were measured on model propellers in inclined flow and in a single-cycle circumferentially non-uniform longitudinal velocity field. The experimental results were correlated with predictions by the following methods:

1. A quasi-steady procedure developed by McCarthy at David W. Taylor Naval Ship Research and Development Center (DTNSRDC),
2. An unsteady lifting surface theory developed by Tsakonas and his colleagues at Davidson Laboratory,
3. An unsteady lifting surface theory developed by Kerwin and Lee at MIT,
4. A refinement by Kerwin to the method of Kerwin and Lee to consider the inclination of the propeller slipstream.

In inclined flow, all four of the calculation methods evaluated consistently underpredicted the experimental values of the periodic single-blade loads. The method of Kerwin, which considers the inclination of the slipstream relative to the propeller axis, produced the best correlation with experimental values. These correlations show that the inclination of the propeller slipstream relative to the propeller axis significantly influence the periodic single-blade loads. The importance of this inclination increases with increasing timeaverage loading.

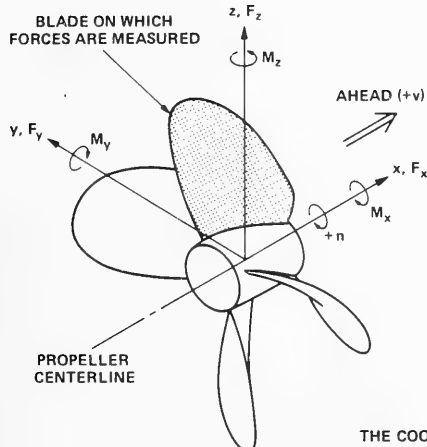
In longitudinal flow, all of the calculation procedures predicted periodic singleblade axial force at design advance coefficient to within 20 percent of the experimental values, but agreement was not as good at off-design advance coefficients. The method of Kerwin and Lee produced the best overall correlation with experimental results considering both amplitude and phase of the periodic single-blade axial force over a range of advance coefficients.

NOMENCLATURE

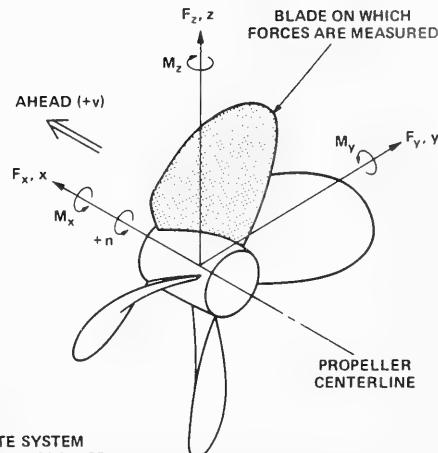
A_E	Expanded area, $\int_{r_h}^R z \text{ cdr}$
A_0	Propeller disk area, $\pi D^2/4$
c	Blade section chord length

D	Propeller diameter
$F_{x,y,z}$	Force components on blade in x,y,z directions
J	Advance coefficient, $J = V_A/nD$
K_Q	Torque coefficient, $Q/(pn^2D^5)$
K_T	Thrust coefficient, $T/(pn^2D^4)$
$M_{x,y,z}$	Moment components about x,y,z axes loading on one blade
n	Propeller revolutions per unit time
P	Propeller blade section pitch
Q	Time-average propeller torque arising from loading on all blades, $-zM_x$
R	Radius of propeller
r	Radial coordinate from propeller axis
T	Time-average thrust of propeller, positive forward, zF_x
V	Model speed
V_A	Propeller speed of advance
$V_r(r, \theta_w)$	Radial component of wake velocity, positive towards hub
$V_t(r, \theta_w)$	Tangential component of wake velocity, positive clockwise looking upstream for left-hand propeller, positive counter-clockwise looking upstream for right-hand propeller
$V_x(r, \theta_w)$	Longitudinal component of wake velocity, positive forward
V_{VM}	Volume mean longitudinal velocity through propeller disk determined from wake survey

\bar{V}_{VM}	Wake fraction determined from volume mean longitudinal velocity through propeller disk determined from a wake survey, $(V - \bar{V}_{VM})/V$	REF	Value at specified reference advance coefficient
x, y, z	Coordinate axes	x, y, z	Component in x, y, z direction
Z	Number of blades	<u>Superscripts:</u>	
θ	Angular coordinate used to define location of blade and variation of loads, from vertical upward, positive counterclockwise looking upstream for left-hand propeller, positive clockwise looking upstream for right-hand propeller, $\theta = -\theta_w$	-	Time-average value per revolution
θ_w	Angular coordinate of wake velocity, from upward vertical, positive clockwise looking upstream for left-hand propeller, positive counterclockwise looking upstream for right-hand propeller, $\theta_w = -\theta$		
$\kappa_{(F)n}$	nth harmonic force coefficient, $(F)_n / (\rho n V_A D^3)$		
$\kappa_{(M)n}$	nth harmonic moment coefficient, $(M)_n / (\rho n V_A D^4)$		
	Mass density of water		
$(\phi_{F,M})_n$	nth harmonic phase angles of F, M based on a cosine series, $(F, M) = (\bar{F}, \bar{M}) + \sum_{n=1}^N (F, M)_n \cdot \cos(n\theta - (\phi_{F,M})_n)$		
ψ	Inclination of propeller shaft		
<u>Subscripts:</u>			
d	Value at the near design condition		
EXP	Value of experimental measurements		The experimental results were correlated with predictions by the following theoretical methods:
h	Value of hub radius		1. A simple quasi-steady procedures developed by McCarthy (5) at DTNSRDC which utilizes the open
n	Value of nth harmonic		



COORDINATE SYSTEM FOR RIGHT HAND PROPELLER
(PROPELLERS 4710 and 4402)



COORDINATE SYSTEM FOR LEFT HAND PROPELLER
(PROPELLER 4661)

Fig. 1 – Components of Blade Loading

water characteristics of the propeller,

2. A linearized lightly-loaded unsteady lifting surface theory developed by Tsakonas, et al (6,7) at Davidson Laboratory,
3. A moderately-loaded unsteady lifting surface theory developed by Kerwin and Lee (8) at MIT,
4. A refinement by Kerwin (9) to the method of Kerwin and Lee which considers the inclination of the propeller slipstream for operation in inclined flow.

BACKGROUND

In previous work unsteady loads (see Figure 1) were measured on a single blade of model propellers operating behind model hulls with open-shaft transom sterns (1,2,3,4). It was found that for these vessels the unsteady blade loads were produced primarily by the tangential component of the wake velocity; see Figure 2. For the steady ahead conditions, the experimentally obtained unsteady loads were correlated with unsteady loads deduced from strains measured on the respective full scale propeller blades and with predictions based on unsteady lifting surface theory developed by Tsakonas, et al (6,7), and the quasi-steady method of McCarthy (5).

For each of these propeller-hull combinations, the circumferential

variation of loading determined from the model experiments agreed fairly well with full-scale data, but was substantially larger than the predictions by the two theoretical methods.

In an attempt to isolate the reasons for the large discrepancy between these experimental and theoretical results, the following experimental work on model propellers was undertaken:

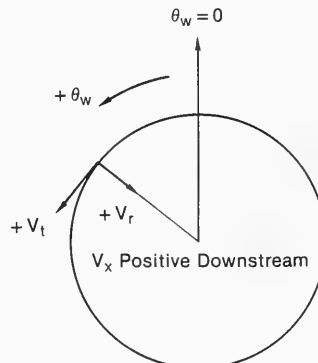


Fig. 2 – Sign Convention for Ship Wake Velocity Components

1. Measurement of the six components of blade loading under various idealized conditions including:
 - a. In inclined flow without an upstream hull.
 - b. In a once-per-revolution variation of longitudinal flow produced by an upstream wire-grid screen.
 - c. Over a range of propeller advance coefficients.
 - d. Over a range of clearances between the propeller tip and a flat plate above the propeller.
2. Measurement of the field point velocities induced by a propeller operating in inclined flow.
3. Measurement of the pressure distribution on the surfaces of the blades of two propellers operating in inclined flow.

This paper presents the results of the blade loading experiments under idealized conditions, and correlation with available theories including one which considers the influence of slipstream for operation in inclined flow. These results supersede the preliminary results presented in Reference 10. More details of these results will be presented in future DTNSRDC Reports. The field point velocity measurements were reported in Reference 11. The results of the blade surface pressure measurements will be presented in a future DTNSRDC Report.

EXPERIMENTAL TECHNIQUES

The experiments were conducted on DTNSRDC Carriage 2. The propellers were mounted at the front of the downstream drive system containing the dynamometer and the drive motor. This system was the same as that used in the experiments described in detail in References 2 and 3 except that the downstream body was modified so that it could be operated fully submerged. The modifications included a waterproof housing for the drive motor, waterproof electrical cables and connectors, removal of the upper apron which had extended the sides of the boat, and the addition of a non-waterproof top to the boat.

The sensing elements were flexures to which bonded semi-conductor strain-gage bridges were attached. Three flexures were necessary to measure all six components of forces and moments. Flexure 1 measured F_x and M_y , Flexure 2 measured F_y and M_x , and Flexure 3 measured F_z and M_z ; see Figure 1. The flexures were mounted

inside a propeller hub specifically designed for these experiments. Only one flexure could be mounted at a time because of space limitations, and this necessitated three duplicate runs for each condition. The flexure calibration procedure was identical to that described in References 2 and 3.

Wake Screen and Wake Survey

A 16-inch (0.405 m) diameter wake screen designed to produce a dominant first harmonic of the circumferential variation of the axial velocity, was used in the experiments. This screen consisted of simply a base screen with one overlay screen and no support members in the region through which flow is drawn into the propeller disk.

Wakes were measured for three different flow regimes:

1. Shaft inclination $\psi = 10$ deg with no wake screen,
2. $\psi = 20$ deg with no wake screen,
3. $\psi = 0$ deg with the wake screen.

Figure 3 shows the velocity component ratios at the radial position near $r=0.7R$ at which the various wake surveys were conducted. The circumferential variations of the velocity component ratios in the axial, tangential, and radial directions contained primarily first harmonic components.

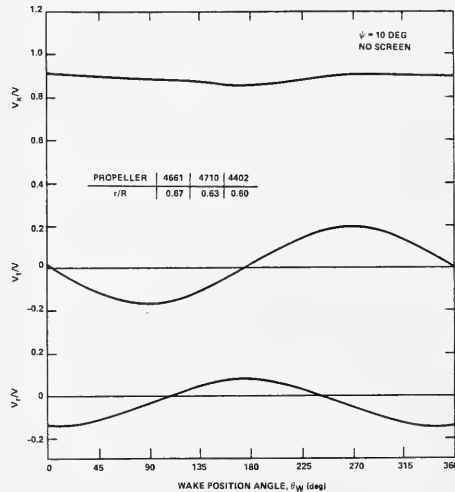


Fig. 3 – Distribution of Wakes in Propeller Disks

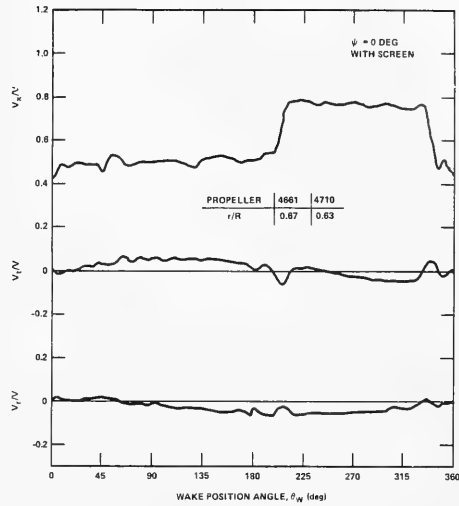
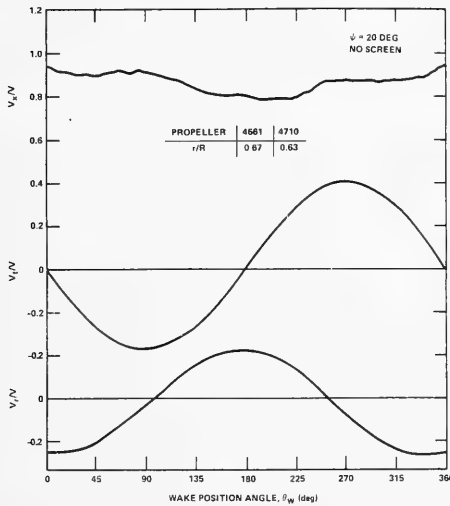


Fig. 3 – (Continued)

Figure 3 shows that the variation of the longitudinal velocity component ratio V_x/V behind the wake screen is approximately a step function, as was expected. However, the high velocity region covers a smaller portion of the propeller disk than the low velocity region, whereas it was anticipated that the two velocity regions would each cover essentially half of the disk. This suggests that there is some cross flow between the propeller and the screen. This non-symmetry of the wake profile causes no problem regarding the objectives of the present investigation since it remains the same for all experimental conditions.

Experimental Conditions and Procedures

The propeller was located approximately 16 in (0.41 m) downstream of the screen for all conditions for which the screen was used. A 4.0 ft by 2.0 ft by 0.375 in (1.22 m by 0.61 m by 9.5 mm) plate was positioned parallel to the flow above the propeller for all experimental conditions. For Propeller 4402 at 10 degrees inclination, the plate clearance from the tip of the propeller was varied from 1.0 in (0.025 m) to 20 in (0.51 m). For all other conditions the plate clearance was approximately 20 in (0.51 m). With this clearance, the plate was 2 in (0.051 m) below the water surface. The plate at this location was used to minimize any possible effects of the free surface on the propeller performance.

The experimental conditions are as follows:

1. No Wake Screen, $\psi = 10$ deg, Propellers 4661, 4710, and 4402.
2. No Wake Screen, $\psi = 20$ deg, Propellers 4661, and 4710.
3. Wake Screen, $\psi = 0$ deg, Propellers 4661 and 4710.
4. No Wake Screen, $\psi = 30$ deg, Propeller 4661.

For each condition, the carriage speed was held constant and propeller rotation speed, n , was varied to obtain the desired range of advance coefficient, J . For each condition, the carriage speed for the blade loading measurements was the same as the carriage speed for the corresponding wake survey.

The first three conditions represent the more important types of experiments performed. The wake surveys were conducted at these conditions. The fourth condition was run to obtain limited data at a very large value of ψ so that the variation of loads with ψ could be better defined. Due to limited time, however, only the F_x and M_y components were measured on Propeller 4661, and no measurements were made on Propeller 4710. In addition, no wake survey was conducted at this condition due to limitations of the wake survey apparatus.

For each of these conditions, experiments were conducted over a range of advance coefficient J . For each

condition, between 20 and 40 values of advance coefficient were evaluated in order to well define the manner in which the loading varies with advance coefficient. In general, each experimental condition was run three times, once for each of the three flexures. This was necessary in order to obtain all six components of force and moment. Data were also collected with the propellers rotating in air at 0, 10, 20, and 30 degrees of shaft inclination over the range of rotational speeds evaluated in water. This provided the gravitational and centrifugal loads that were later subtracted from the total propeller blade loads measured in water.

Data Acquisition and Analysis

Data were collected and analyzed in the same manner as in the steady ahead runs described in References 1 through 4. For each flexure, an Interdata 70 Computer was used to collect and average the force and moment data for each 4-degree increment of blade angular position over 200 to 300 propeller revolutions. Propeller rotation speed, n , and model (or carriage) velocity, V , were recorded for every set of two propeller revolutions, and averaged over the period during which data were collected.

At the end of each run, the computer analyzed and printed the data. The average force and moment signals for each 4-degree angular position were printed along with the average model velocity and propeller rotation speed for the run. The standard deviation of the accumulated data for the run was also calculated for V , n , and the force and moment signals at each position. A harmonic analysis was performed on the force and moment data providing the mean signal and amplitude and phase of the first 16 harmonics.

First, the experimental agenda was completed for all three flexures at each major condition (each propeller, wake screen, and value of ψ) except $\psi = 30$ deg. Then the corrections for interactions were calculated at five values of J at which measurements with all three flexures were made using the same procedures outlined in Reference 1 through 4. After the correction for interactions, the centrifugal and gravitational loads were subtracted from the total experimental loads to obtain the hydrodynamic loads.

Accuracy

The accuracy of the experiment was generally similar to that of the steady ahead runs in References 1 through 4. During a single run, where signals were averaged over many revolutions, the standard deviation of the measured forces and moments maintained a similar error (95 percent confidence band) of ± 5 to ± 10 percent of the averaged signal at each angular position. For a given run the average error in model speed V was approximately ± 1.0 percent, and the error in rotational speed n was less than ± 0.01 percent.

Except for the fluctuations in signals occurring in a given run, the accuracy of the data is indicated by the repeatability of an identical condition. An effort was made to set experimental conditions identically on repeat runs; however, some variation was unavoidable due to manual setting of the model speed and propeller rotation speed, random zero shift in data channels, and minor variations in basin water conditions. This resulting error is approximately ± 2 percent of the measured first harmonic loading component. A more detailed error analysis based on the repeatability of the hydrodynamic, centrifugal and gravitational loads will be presented in a future DTNSRDC Report.

EXPERIMENTAL RESULTS

Loading Components

The basic loading components are shown in Figure 1. For a right-hand propeller the sign convention follows the conventional right-hand rule with right-hand Cartesian coordinate system. For a left-hand propeller all the loads are the same, but for this case the sign convention follows a left-hand rule with a left-hand Cartesian coordinate system.

Each component of loading is generally represented as a variation of the instantaneous values with blade angular position, θ , and as a Fourier series in blade angular position in the following form:

$$F, M(\theta) = (\bar{F}, \bar{M}) + \sum_{n=1}^N (F, M)_n \cos\{\theta - (\phi_{F, M})_n\} \quad (1)$$

In general, the loads consist of hydrodynamic, centrifugal and gravitational components. However, in this

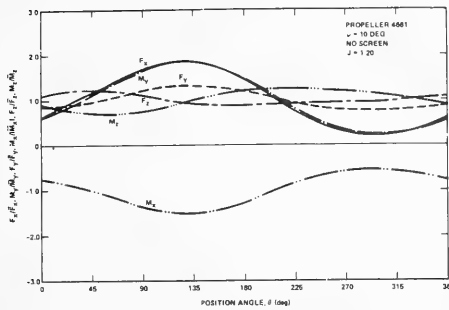


Fig. 4 – Experimental Variation of Loading Components with Blade Angular Position

paper only the hydrodynamic component of blade loading is presented. Centrifugal and gravitational loads were measured solely to permit the hydrodynamic loads to be determined by subtracting the centrifugal and gravitational loads from the total experimental loads.

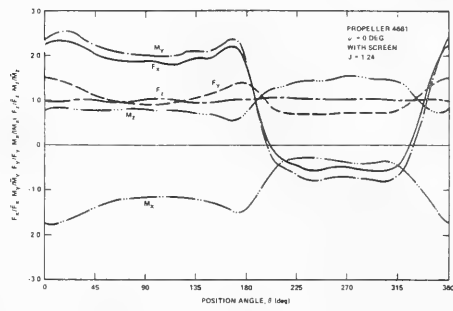
Centrifugal and Gravitational Loads

Centrifugal and gravitational loads were determined from air-spin experiments with each flexure over a range of rotational speed n for $\psi = 0, 10, 20,$ and 30 deg. The centrifugal load, which is a time-average load in a coordinate system rotating with the propeller, should vary as n^2 and be independent of ψ . The time-average experimental data followed these trends closely. The gravitational load, which is a first harmonic load in a coordinate system rotating with the propeller, should vary with ψ and be independent of n . The first harmonic experimental data followed these trends closely.

The centrifugal and gravitational loads measured during these experiments agreed with the values previously reported in References 3 and 4 and the gravitational loads agreed with values deduced from the weights of the blades and associated flexures. Therefore, these results will not be repeated here.

Variation of Loads with Angular Position

Figure 4 shows the variations of the loading components with blade angular position for Propeller 4661 for operation with 10 degrees shaft inclination with no screen and for operation behind the wake screen with no shaft inclination. These plots present typical results obtained in inclined flow and behind the wake screen. For other conditions evaluated in inclined flow and behind the wake screen the trends are basically the same as shown in Figure 4, but the magnitude of the



unsteady loading varies with experimental conditions.

The variations of the primary load components, F_x and M_y with blade angular position in inclined flow and behind the wake screen follow patterns approximately similar to the tangential and the longitudinal velocity profiles of the respective wakes shown in Figure 3. The variation of the loads behind the wake screen implies that the high velocity region covers a smaller portion of the propeller disk than the low velocity region, which agrees with the measured wake data.

Effect of Plate Clearance

Figure 5 shows that the periodic blade loads in inclined flow are fairly insensitive to the presence of a nearby flat boundary parallel to the flow for tip clearance to propeller diameter (tip clearance ratio) as small as 0.1. The ratios of the periodic to the time-average loading components at tip clearance ratio of 0.1 are no greater than 10 percent larger than the

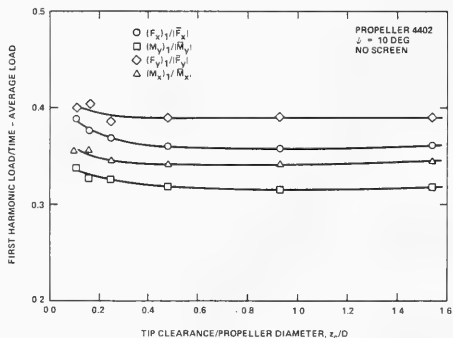


Fig. 5 – Effect of Plate Clearance on First Harmonic Loading in Tangential Wake

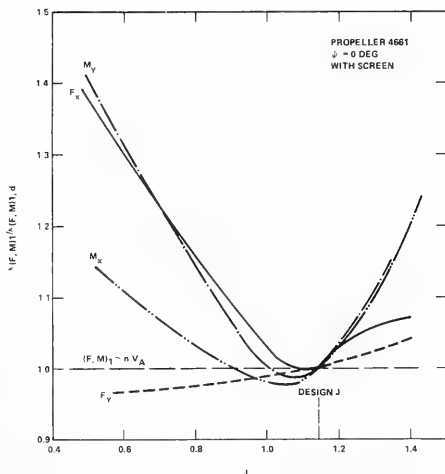
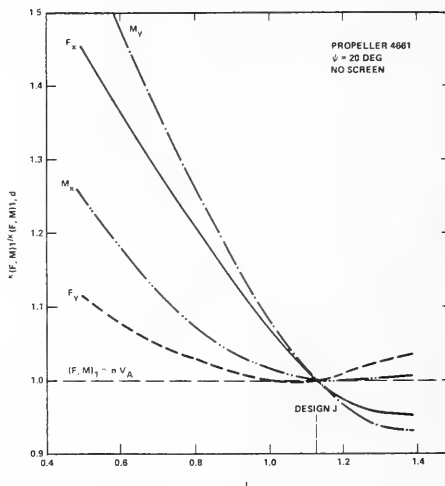
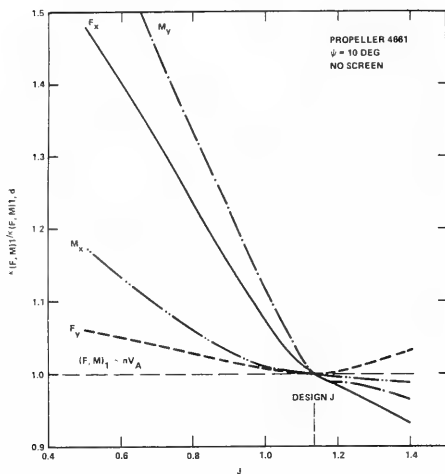


Fig. 6 — Experimental Variation of First Harmonic Blade Loads On Propeller 4661 with Advance Coefficient

corresponding values at very large tip clearance ratios for Propeller 4402 with an inclination angle ψ of 10 degrees.

Effect of Advance Coefficient

Figure 6 presents the trends of the variations of the first harmonics of the primary load components F_x , M_y , F_y , and M_x with J for Propeller 4661 at the three primary experimental conditions described in the section on Experimental Conditions and Procedures.

In Figure 6 the force and moment components are nondimensionalized as follows:

$$\kappa_{(F_x, M_y)_1} = \frac{(F_{x,y})_1}{\rho n V_A D^3} \quad (2)$$

$$\kappa_{(M_{x,y})_1} = \frac{(M_{x,y})_1}{\rho n V_A D^4} \quad (3)$$

where the subscript 1 represents the first harmonic component, and $V_A = V(l-w_M)$ is the speed of advance based on the volume mean wake. This form of nondimensionalization was used in part to verify Wereldsma's argument (12) that for a given propeller in a given wake pattern the circumferential variation of the hydrodynamic loading varies approximately as nV_A ; i.e., for a given value of nV_A the circumferential variation of hydrodynamic loading is insensitive to J . This form of nondimensionalization is different only by a factor of the advance coefficient, J_A , from the conventional form of nondimensionalization; i.e., $F_{x,y}/\rho n^2 D^4$ and $M_{x,y}/\rho n^2 D^5$. The coefficients $\kappa_{(F_x, y)_1}$ and $\kappa_{(M_{x,y})_1}$ in Figure 6 are all normalized by the respective coefficients at design J to illustrate the relative sensitivity of the loading coefficients to J , for different wakes.

The results presented in Figure 6 show that in tangential flow $\kappa_{(F_x, y)_1}$ and $\kappa_{(M_{x,y})_1}$ generally decreases with

increasing J . $\kappa_{(My)1}$ is the most sensitive to J , and $\kappa_{(Fy)1}$ is the least sensitive to J . Except for the F_y component, these data do not closely follow the trends indicated by Wereldsma (12). For the longitudinal wakes behind the screen, the slopes of $\kappa_{(F,M)}$ with increasing J are less negative than in inclined flow. The relative slopes among the four components are generally the same for each propeller-wake combination, except for some cases at greater than design J .

Figure 7 compares the variations of $\kappa_{(Fx)1}$ with J obtained in the present experiment in inclined flow with variations obtained in previous experiments in which the unsteady blade loads were determined over a range of J in inclined flow (13,14,15,16). Each of these sets of experimental results show that $\kappa_{(Fx)1}$ decreases substantially with increasing J .

Figure 8 compares the variation in $\kappa_{(Fx)1}$ with J obtained in the present experiment behind the wake screen with the blade frequency $\kappa_{(Fx)n}$ obtained in previous experiments in

which the unsteady bearing forces were measured in longitudinal wakes produced by screens in a closed-jet water tunnel (17,18,19). The results in References 17, 18, and 19 are for the blade frequency component of κ_{Fx} , whereas in the present investigation the shaft frequency component of κ_{Fx} was measured. However, the mechanism for generating the unsteady blade loading in axial flow appears to be independent of the harmonic of shaft rotation. Each of the three previous sets of experiments shows that $\kappa_{(Fx)n}$ decreases with increasing J to some minimum value near design J , and then increases with further increase in J . Figure 8 illustrates that variations of $\kappa_{(Fx)1}$ with J obtained in the present experiment generally follow the trend of the data in References 17, 18 and 19. In general, $\kappa_{(Fx)n}$ is somewhat less sensitive to J in longitudinal wake patterns than it is in tangential wake patterns.

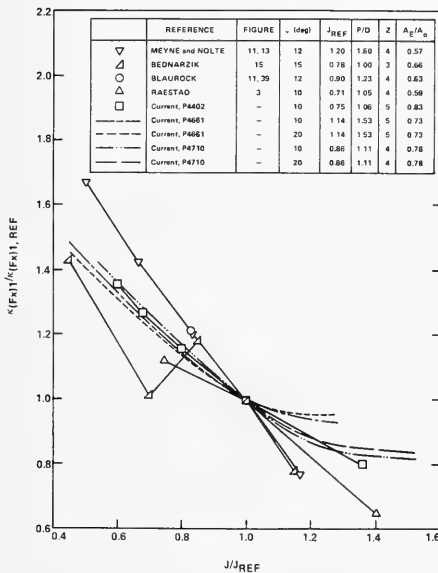


Fig. 7 – Comparison of First Harmonic Blade Loading Coefficients in Tangential Wakes

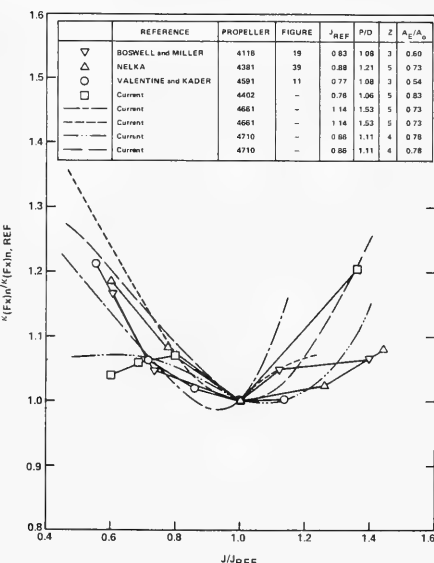


Fig. 8 – Comparison of Various Experimental Blade Loading Coefficients in Longitudinal Wakes

CORRELATION BETWEEN EXPERIMENTAL RESULTS AND THEORETICAL PREDICTIONS

Theoretical Methods

The experimental results were correlated with predictions based on the following methods:

1. The quasi-steady method developed at DTNSRDC by McCarthy (5); Computer Program QUASI.
2. The procedure developed at Davidson Laboratory by Tsakonas, et al (6,7) based on lightly-loaded unsteady lifting surface theory; Computer Program PPEXACT.
3. The procedure developed at MIT by Kerwin and Lee (8) based on moderately-loaded unsteady lifting surface theory; Computer Program PUF2.
4. A refinement of the method of Kerwin and Lee (8) developed at MIT by Kerwin (9), to allow the axis of the propeller slipstream to depart from the propeller axis for operation in inclined flow; Computer Program PUF2IS.

The procedure developed by McCarthy (5) is a simple quasi-steady procedure utilizing the open water characteristics of the propeller. It is assumed that the thrust and torque developed by the propeller blade at any angular position in a circumferentially nonuniform wake is the same as would be produced by the propeller blade if it were operating continuously at the advance coefficient J and rotational speed n based on the local wake at the angular position corresponding to the mid-chord of the 70 percent radius. It is further assumed that the instantaneous thrust and torque can be adequately estimated by entering the propeller open water characteristics at the values of J and n based on a weighted average over the propeller radius of the wake at the local blade angular position. This simple method can be expected to yield reasonable results only if the reduced frequency of interest is low, the propeller projected skew is small relative to the wave length of the pertinent wake harmonic, and the wake harmonic corresponding to the force harmonics of interest does not vary substantially in amplitude or phase with radius. These conditions are met for propellers and wakes being evaluated in the present paper.

The procedure developed by Tsakonas, et al (6,7), is based on the linearized unsteady lifting surface theory for a lightly-loaded propeller using an acceleration potential. The

numerical procedure applies the mode approach and collocation method in conjunction with the "generalized lift operator" technique. This procedure based on the frequency domain assumes that a given harmonic of blade loading depends upon the corresponding harmonic of the wake velocity normal to the blade chord line, independent of whether the normal velocity results from axial or tangential components of the wake. The blade load does not depend upon the radial variation of the circumferential mean wake. The shed and trailing vortices are assumed to lie on an "exact" helicoidal surface of constant pitch extending to downstream infinity determined by the propeller rotational speed and a single axial inflow velocity. The axis of this helicoidal surface coincides with the propeller axis, regardless of the inclination of the propeller shaft to the incoming flow. This method does not consider the contraction or roll-up of the propeller slipstream. All geometric characteristics of the propeller are considered, except rake, camber, and thickness which are assumed to be zero.

Valentine (20) developed a refinement to the method of Tsakonas, et al (6,7) for operation in slightly inclined flow. This refinement, in effect, replaces the "exact" helicoidal wake whose axis coincides with the propeller axis with a slightly distorted one in the direction of the inflow velocity. The refinement, which is incorporated as a perturbation for small inclination angles, relates the unknown loading at the first harmonic of shaft frequency with the loadings at the mean and second harmonics of shaft frequency evaluated without the distorted helicoidal wake. All other assumptions of the method of Tsakonas et al, are retained.

Calculations made by Valentine (20) showed that his modification to the method of Tsakonas et al, did not significantly improve the poor correlation between this method and experimental blade loads in inclined flow. Further, with the modifications by Valentine the disagreement in phase between predicted and experimental blade loads in inclined flow were even worse than the agreement obtained with the method of Tsakonas et al. Valentine concluded that the effects of shaft inclination required a moderately-loaded propeller theory, and could not be adequately calculated based on the lightly-loaded formulation of Tsakonas et al. Therefore, the theory of Tsakonas et al, as modified by Valentine was not correlated with the experimental results in the present paper.

The numerical method developed by Kerwin and Lee (8) is based on a linearized lifting-surface theory in the time domain. The propeller blades are represented by a spanwise and chordwise distribution of discrete line vortex and source elements located on the exact camber surface of the blade. Thus the geometric complications of skew, rake and radial variation in pitch are readily accommodated. The trailing vortex wake is permitted to contract and roll up, and the effect of vortex sheet separation from the blade tip is taken into consideration. The inflow velocity to the propeller may have radially and circumferentially varying axial, tangential, and radial components, and may therefore give rise to both steady and unsteady blade loading. This method, like the method of Tsakonas et al., assumes that the axis of the propeller slipstream coincides with the propeller axis.

Kerwin (9) developed a refinement to the method of Kerwin and Lee (8) for operation in inclined flow where the slipstream is not axisymmetric about the propeller shaft. This refinement entails a more realistic representation of the path of the propeller slipstream. In this method the axis of the slipstream coincides with the propeller axis immediately behind the propeller, and coincides with the direction of the mean inflow far downstream in the ultimate wake. A simple function is assumed for the slipstream axis in the wake region between the propeller and the ultimate wake. Due to the asymmetry, the position of the trailing vortex wake relative to a blade oscillates with a once-per-revolution fundamental frequency, thus giving rise to unsteady induced velocities normal to the blade surface and thereby unsteady blade loadings of the same frequency. The strength of the vorticity in the wake, and thus the induced once-per-revolution variation of loading on the blades, is dependent upon the time-average loading of the propeller. All other characteristics of the method of Kerwin and Lee except for roll-up are retained, including the flexibility for the trailing vortex wake to contract, and allowance for the effect of vortex sheet separation from the blade tip.

Correlations in Tangential Wakes

Figures 9 and 10 present the amplitudes and phases, respectively, of the first harmonic loads on Propellers 4661, 4710, and 4402 operating in the various tangential wakes over a range of

advance coefficient J . These figures present both experimental results and predictions based on the various theoretical methods described in the preceding section. For Propeller 4661 with 10 degrees shaft inclination, the first harmonic components of F_x , M_y , F_y , and M_x are presented. For other conditions only the F_x component is shown. The results in Figure 9 and 10 are summarized in Table II for design J.

In the tangential wakes, a consistent variation from the experimental data occurred in the theoretical predictions for the three propellers evaluated. With few isolated exceptions, all of the theoretical methods underpredicted all of the loading components throughout the range of conditions evaluated. In general, the correlations are better for the F_x and M_y components than for the F_y and M_x components. The F_x and M_y components are the more important components since, in general, these are larger than the F_y and M_x components.

The quasi-steady method of McCarthy (5) underpredicted the amplitude of $(F_x)_1$ by approximately 10 to 30 percent of the experimental values with closer agreement at higher values of J . The quasi-steady predictions maintained a similar trend to the experimental data for F_x and M_x components for all conditions in tangential wakes; i.e., both the experimental and predicted values of $\langle F_x \rangle_1$ and $\langle M_x \rangle_1$ decrease with increasing J . For a given propeller the predicted slope of the $\langle F_x \rangle_1$ and $\langle M_x \rangle_1$ curves (not shown) with J increases with increasing amplitude of the tangential wake. No predictions of $(F_y)_1$ and $(M_y)_1$ were made with the quasi-steady procedure since this method does not predict the radial center of the load. These components could be predicted by the quasi-steady method by assuming a radial position of application of the load.

The phases presented in Figure 10 show that the quasi-steady method of McCarthy predicts that the maximum values of the loading components will occur at approximately 10 to 20 degrees of blade angular position before the experimentally determined angles.

Predictions by the unsteady theory of Tsakonas et al (6,7) did not agree well with experimental results in tangential flow. This theory predicts that the amplitudes of all four loading coefficients increase with increasing J ,

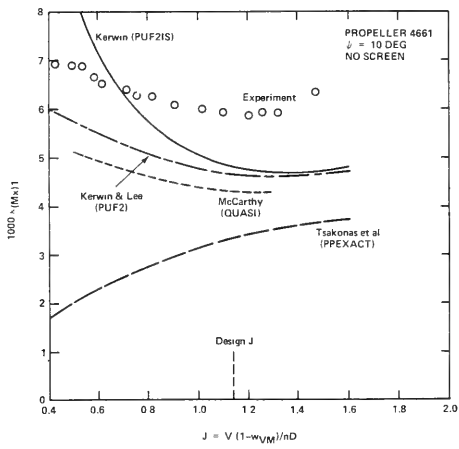
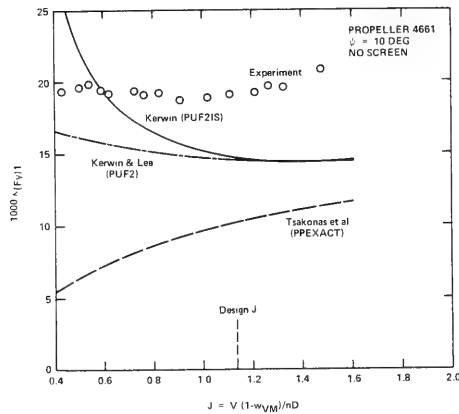
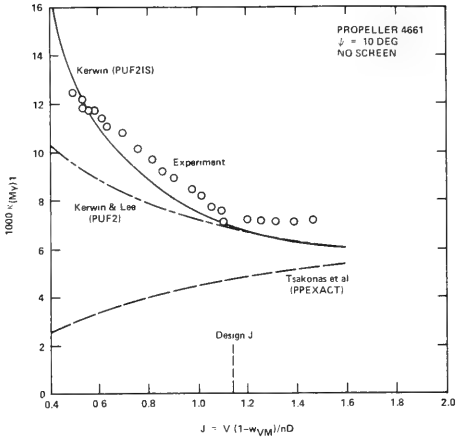
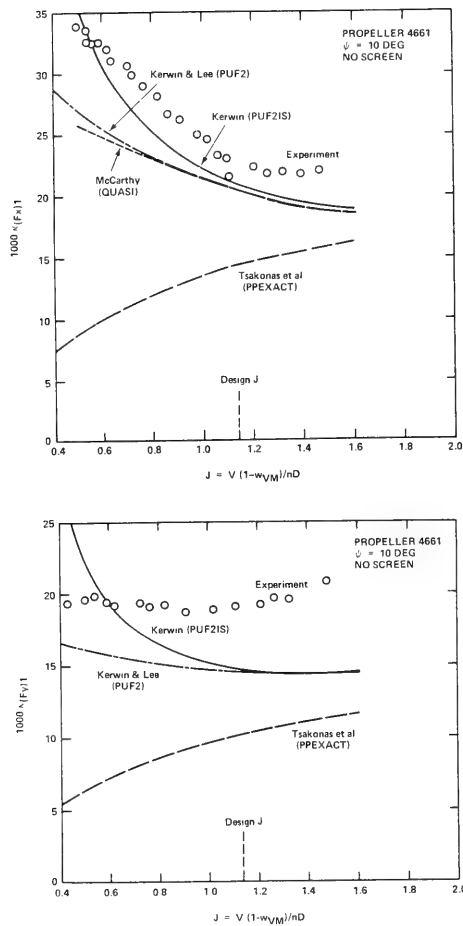


Fig. 9 – Amplitudes of First Harmonic Blade Loads in Tangential Wakes; Correlation Between Experiment and Theory

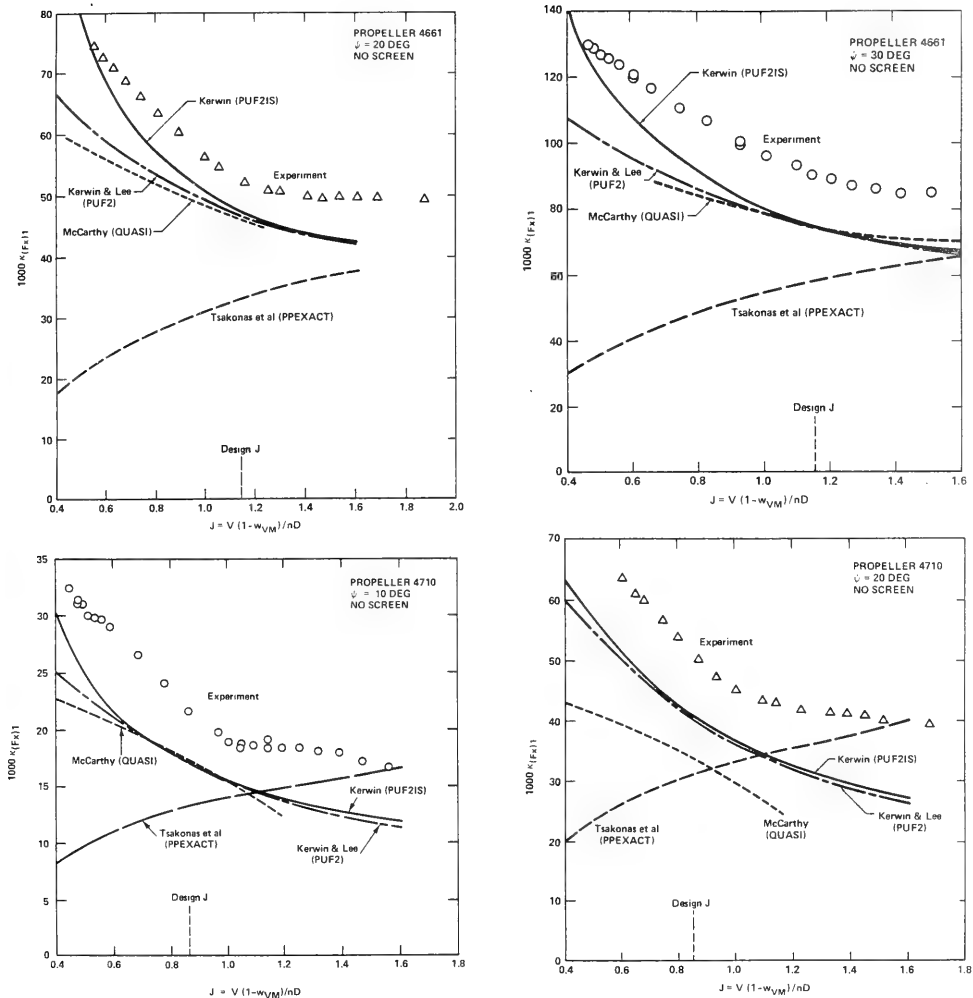


Fig. 9 – (Continued)

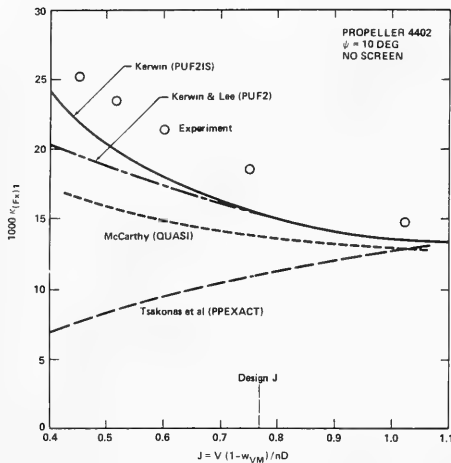


Fig. 9 -- (Continued)

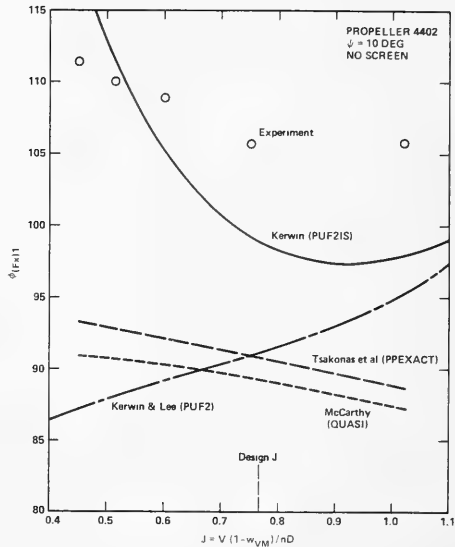


Fig. 10 -- Phases of First Harmonic Blade Loads in Tangential Wakes Correlation Between Experiment and Theory

which is opposite to the trend of the experimental data. Since this is a lightly-loaded linear theory, it was anticipated that the predicted unsteady loading coefficients $K(F, M)_1$ would be essentially independent of J . An earlier version of the unsteady lifting surface method developed by Tsakonas and his associates (21) at Davidson Laboratory, in which the propeller helical wake was approximated in a staircase manner did predict that the periodic loading coefficients $K(F, M)$ in axial wakes were essentially independent of J (17). It is not clear why the method of Tsakonas et al (6,7) predicts that $K(F, M)_1$ increases substantially with increasing J .

In general, the predictions by the method of Tsakonas et al are closer to the experimental results at high advance coefficients than they are at low advance coefficients. The predicted amplitudes are approximately 65 percent of the experimental value at design J and 30 to 35 percent of the experimental values at the lowest values of J evaluated. The finding that this method predicts periodic loads in inclined flow that are significantly less than the experimental values is consistent with the results presented in References 1 through 4.

The unsteady theory of Tsakonas et al predicts that the maximum values of the loading components will occur at approximately 15 to 20 degrees of blade angular position before the experimentally determined angles; see Figure 10.

The unsteady theory of Kerwin and Lee (8) showed, in general, somewhat better agreement with experimental data over a range of advance coefficient than either the quasi-steady method of McCarthy or the unsteady method of Tsakonas et al. This applies to both amplitudes and phases. The trends of the predictions of the amplitudes over a range of advance coefficients were very similar to the trends of the predictions by the method of McCarthy. The method of Kerwin and Lee underpredicted the periodic loads, by approximately 5 to 20 percent of the experimental values, with closer agreement being obtained for the F_x and M_y components at the higher values of J .

The unsteady theory of Kerwin and Lee predicts the phases to within 5 to 15 degrees of the experimental values

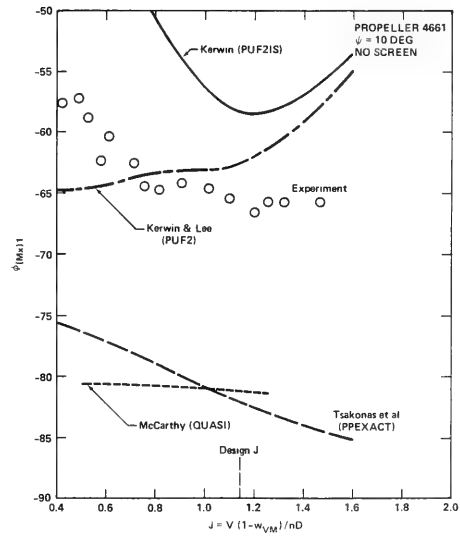
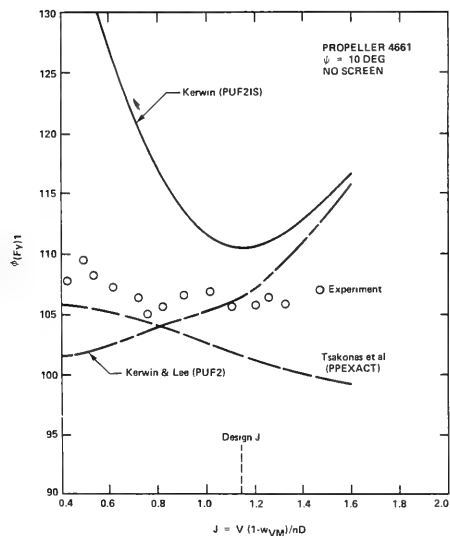
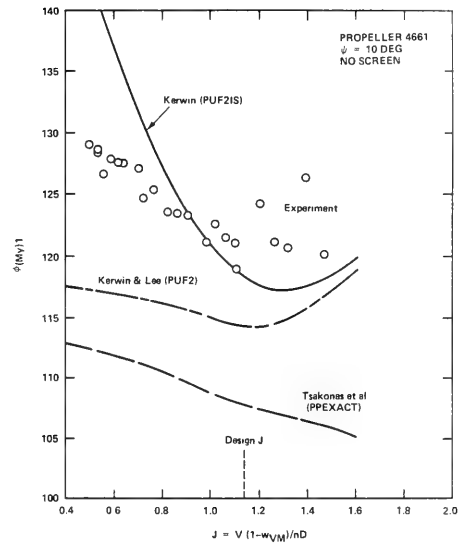
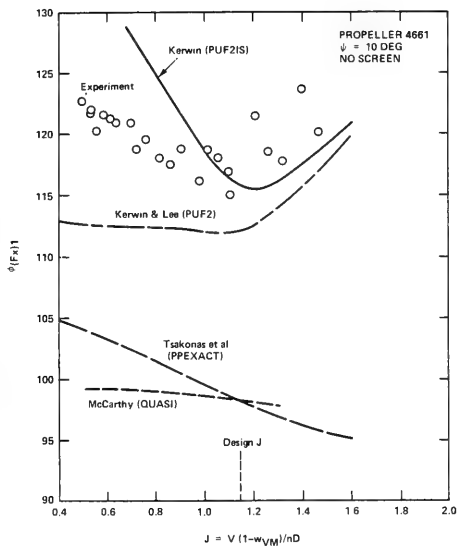


Fig. 10 -- (Continued)

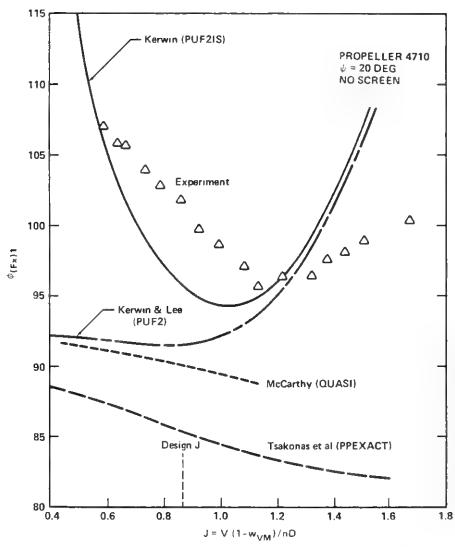
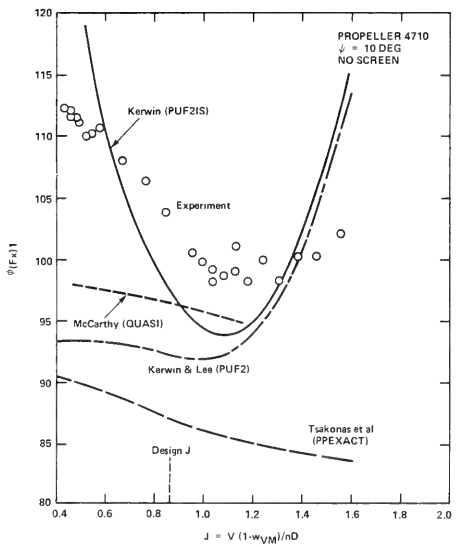
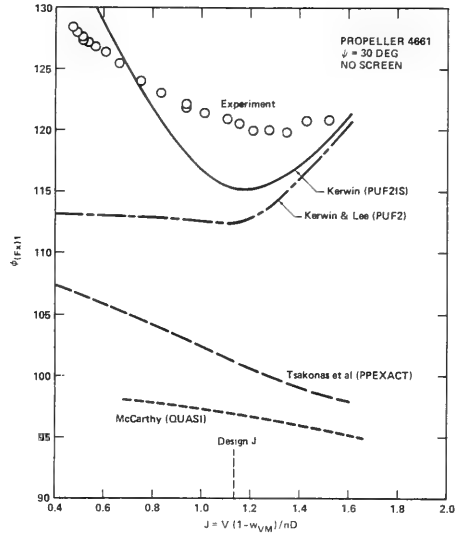
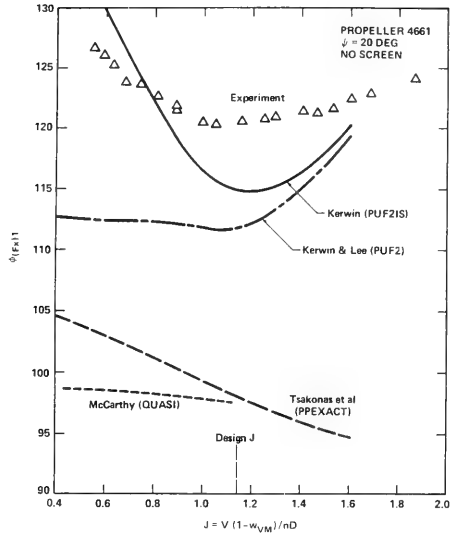


Fig. 10 – (Continued)

TABLE II – COMPARISON OF EXPERIMENT AND THEORY IN INCLINED FLOW – AMPLITUDES AND PHASES OF FIRST HARMONIC LOADING COEFFICIENTS AT DESIGN J

PROPELLER 4661, $\psi = 10$ DEG, J = 1.14								
AMPLITUDE	$1000 \cdot \frac{K_{(Fx)1}}{K_{(Fx)1}}$	$\frac{K_{(Fx)1}}{K_{(Fx)1}, EXP}$	$1000 \cdot \frac{K_{(My)1}}{K_{(My)1}}$	$\frac{K_{(My)1}}{K_{(My)1}, EXP}$	$1000 \cdot \frac{K_{(Fy)1}}{K_{(Fy)1}}$	$\frac{K_{(Fy)1}}{K_{(Fy)1}, EXP}$	$1000 \cdot \frac{K_{(Mx)1}}{K_{(Mx)1}}$	$\frac{K_{(Mx)1}}{K_{(Mx)1}, EXP}$
Experiment	23.00		7.50		19.10		5.90	
McCarthy (QUASI)	20.50	0.89	—	—	—	—	4.31	0.73
Tsakonas et al (PPEXACT)	14.50	0.63	4.80	0.64	10.36	0.54	3.34	0.57
Kerwin and Lee (PUF2)	20.35	0.88	6.75	0.90	14.47	0.76	4.65	0.79
Kerwin (PUF2IS)	20.79	0.90	6.93	0.92	14.74	0.78	4.82	0.82

PHASE ANGLE	$\phi_{(Fx)1}$	$\phi_{(Fx)1} - \phi_{(Fx)1, EXP}$	$\phi_{(My)1}$	$\phi_{(My)1} - \phi_{(My)1, EXP}$	$\phi_{(Fy)1}$	$\phi_{(Fy)1} - \phi_{(Fy)1, EXP}$	$\phi_{(Mx)1}$	$\phi_{(Mx)1} - \phi_{(Mx)1, EXP}$
Experiment	117.0		120.4		106.0		-65.8	
McCarthy (QUASI)	98.3	-18.7	—	—	—	—	-81.2	-15.4
Tsakonas et al (PPEXACT)	98.2	-18.8	107.8	-12.6	101.8	-4.2	-82.0	-16.2
Kerwin and Lee (PUF2)	112.0	- 5.0	114.2	- 6.2	106.3	0.3	-62.8	3.0
Kerwin (PUF2IS)	115.7	- 1.3	118.1	- 2.3	110.3	3.7	-58.6	7.2

*All phase angles are in degrees.

CONDITION	PROPELLER 4661 $\psi = 20$ DEG	PROPELLER 4661 $\psi = 30$ DEG	PROPELLER 4710 $\psi = 10$ DEG	PROPELLER 4710 $\psi = 20$ DEG	PROPELLER 4402 $\psi = 10$ DEG			
AMPLITUDE	$1000 \cdot \frac{K_{(Fx)1}}{K_{(Fx)1}}$	$1000 \cdot \frac{K_{(Fx)1}}{K_{(Fx)1}, EXP}$	$1000 \cdot \frac{K_{(Fx)1}}{K_{(Fx)1}}$	$1000 \cdot \frac{K_{(Fx)1}}{K_{(Fx)1}, EXP}$	$1000 \cdot \frac{K_{(Fx)1}}{K_{(Fx)1}}$			
Experiment	53.00	91.00	21.80	50.43	18.10			
McCarthy (QUASI)	46.20	0.87	75.00	0.82	33.70	0.67	13.70	0.76
Tsakonas et al (PPEXACT)	33.33	0.63	58.30	0.64	31.55	0.63	11.00	0.61
Kerwin and Lee (PUF2)	46.58	0.88	74.47	0.82	39.92	0.79	15.45	0.85
Kerwin (PUF2IS)	47.28	0.89	75.44	0.83	40.20	0.80	15.47	0.85

PHASE ANGLE	$\phi_{(Fx)1}$	$\phi_{(Fx)1} - \phi_{(Fx)1, EXP}$						
Experiment	120.5		120.6		103.8		102.0	
McCarthy (QUASI)	97.5	-23.0	96.9	-23.7	96.5	- 7.3	90.1	-11.9
Tsakonas et al (PPEXACT)	98.1	-22.4	101.1	-19.5	87.2	-16.6	85.5	-16.5
Kerwin and Lee (PUF2)	111.7	- 8.8	112.4	- 8.2	92.0	-11.8	91.5	-10.5
Kerwin (PUF2IS)	114.8	- 5.7	115.2	- 5.4	97.7	- 6.1	96.0	- 6.0

for most conditions evaluated. In general, the agreement is better for the higher values of advance coefficient J ; i.e., J near or higher than the design value.

The method of Kerwin (9), which is a refinement to the method of Kerwin and Lee to account for the effect of the inclined slipstream, showed substantial improvement over the predictions of amplitudes and phases by the method of Kerwin and Lee at values of J which are substantially less than the design J . For higher J values, i.e., J near or higher than the design value, where the method of Kerwin and Lee was in closer agreement with experimental results, the improvement by the method of Kerwin was smaller. This implies that the influence of the non-axi-symmetric wake due to shaft inclination on the fluctuating forces becomes larger at lower values of advance coefficient. This trend is expected, as pointed out by Kerwin (9), since the effect of wake asymmetry is the combined result of the time-average loading and the oscillating position of the trailing vortex wake relative to a point fixed on the blade. At low advance coefficients, the mean loading is higher, and the pitch of the trailing vortex wake is smaller. This smaller pitch of the propeller wake tends to increase the influence of the fluctuating wake position relative to the blade on induced velocities since the downstream wake is closer to the propeller blades.

In summary, these correlations show that the inclination of the propeller slipstream relative to the propeller axis can significantly influence the periodic loads on the propeller blades. The importance of this inclination increases with increasing time-average loading. Of the four methods evaluated, the method of Kerwin, which accounts for the inclination of the slipstream, gives the best predictions of the amplitudes and phases of the periodic blade loads. The method of Tsakonas et al gives the worst prediction of the amplitudes of the periodic loads. Further, this method failed to predict the trend of the variation of the loading coefficients with advance coefficient.

Figure 11 presents the variation of the periodic loads with inclination angle for Propeller 4661 near design J . These results show that the rate of increase of the periodic loads with inclination angle increases with increasing inclination angle. Figure 11 also shows that the correlation between experimental results and analytical

method of Kerwin, which considers the inclination of the propeller slipstream, is essentially independent of the angle of inclination up to 30 degrees.

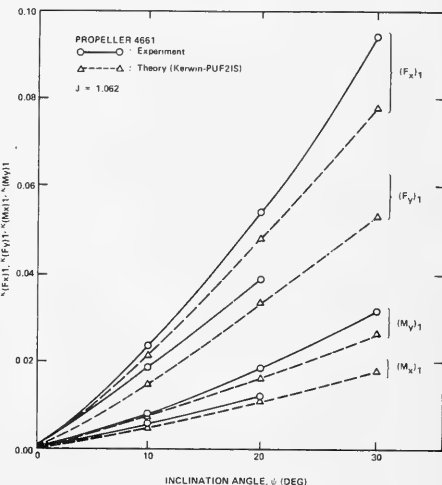


Fig. 11 – Variation of Periodic Blade Loads with Shaft Inclination

Correlations in Longitudinal Wakes

Figures 12 and 13 present the amplitudes and phases, respectively, of the first harmonic of the F_x component on Propellers 4661 and 4710 in the longitudinal wake patterns generated by the upstream wake screen over a range of advance coefficient J . The circumferential variation of the longitudinal component of the incoming velocity is essentially a once-per-revolution variation with low velocity on the left half of the propeller disk and high velocity on the right side of the propeller disk looking upstream; see Figure 3. Figures 12 and 13 also present the correlation between experimental results and predictions based on the three theoretical methods described previously.* The results in Figures 12 and 13 are summarized in Table III for design J .

*For longitudinal inflow where $\psi = 0$, the method of Kerwin (9) is identically the same as the method of Kerwin and Lee (8).

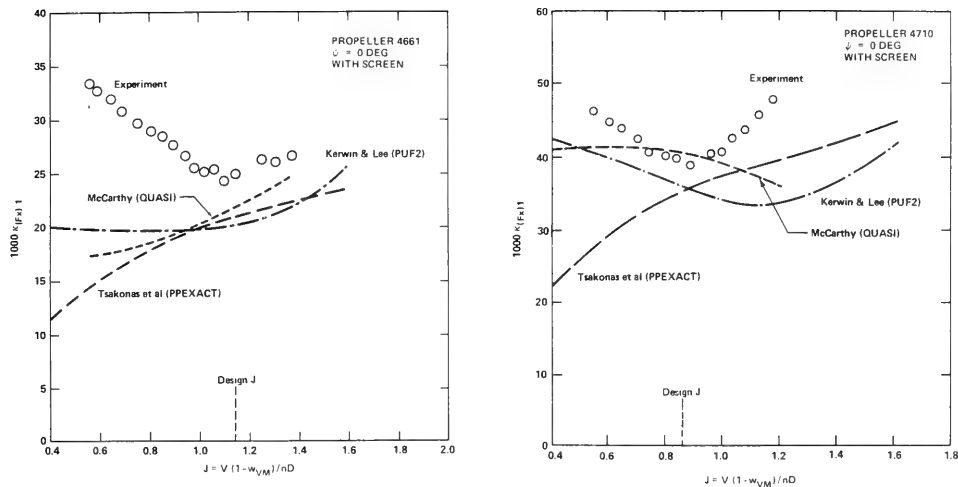


Fig. 12 – Amplitudes of First Harmonic Blade Loads in Longitudinal Wakes; Correlation Between Experiment and Theory

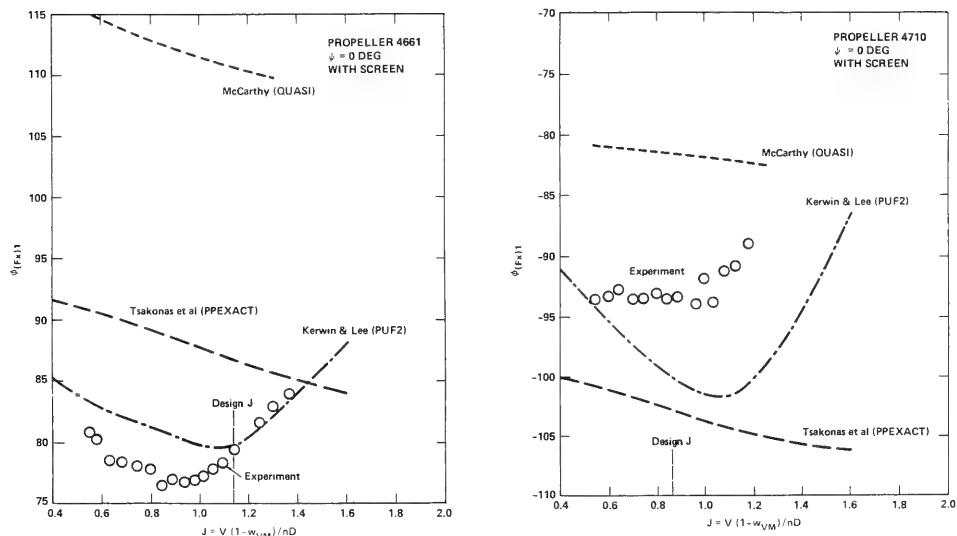


Fig. 13 – Phases of First Harmonic Blade Loads in Longitudinal Wakes; Correlation Between Experiment and Theory

TABLE III – COMPARISON OF EXPERIMENT AND THEORY IN LONGITUDINAL FLOW – AMPLITUDES AND PHASES OF FIRST HARMONIC LOADING COEFFICIENTS AT DESIGN J

CONDITION	PROPELLER 4661 $\psi = 0$ DEG		PROPELLER 4710 $\psi = 0$ DEG	
	$1000 \cdot \frac{\kappa_{(Fx)1}}{\kappa_{(Fx)1, EXP}}$	$\phi_{(Fx)1} - \phi_{(Fx)1, EXP}$	$1000 \cdot \frac{\kappa_{(Fx)1}}{\kappa_{(Fx)1, EXP}}$	$\phi_{(Fx)1} - \phi_{(Fx)1, EXP}$
Experiment	24.92		39.60	
McCarthy (QUASI)	21.70	0.87	40.50	1.02
Tsakonas et al (PPEXACT)	21.00	0.84	35.50	0.90
Kerwin and Lee (PUF2)	19.91	0.80	36.00	0.91

PHASE ANGLE	$\phi_{(Fx)1}$	$\phi_{(Fx)1} - \phi_{(Fx)1, EXP}$	$\phi_{(Fx)1}$	$\phi_{(Fx)1} - \phi_{(Fx)1, EXP}$
Experiment	79.4		- 93.2	
McCarthy (QUASI)	110.6	31.2	- 81.6	11.6
Tsakonas et al (PPEXACT)	86.8	7.4	-102.7	-9.5
Kerwin and Lee (PUF2)	79.6	0.2	-100.0	-6.8

The experimental curve presenting $\kappa_{(Fx)1}$ versus advance coefficient J shows a concave shape with a minimum value near design J ; see Figure 12. The same trend was observed for other loading components (not shown). All of the theoretical methods are in good agreement with experimental $\kappa_{(Fx)1}$ near design J ; however, they did not, in general, agree well with experimental $\kappa_{(Fx)1}$ over a wide range of J . The correlations between experiments and theoretical predictions are somewhat different for the two propellers.

The predictions by the quasi-steady method of McCarthy showed different trends for different propellers. For Propeller 4661, the predicted values of $\kappa_{(Fx)1}$ and $\partial\kappa/\partial J$ increase with increasing J . For Propeller 4710, however, the predicted values of $\kappa_{(Fx)1}$ and $\partial\kappa/\partial J$ decrease with increasing J . The trends of the predictions by the quasi-steady method of McCarthy are quite sensitive to small changes in the slopes of the open water curves; i.e. \bar{K}_T versus J and \bar{K}_Q versus J .

The phases shown in Figure 13 show that the quasi-steady method of McCarthy predicts that the maximum value of $(Fx)_1$, will occur at approximately

25 and 10 degrees of blade angular position after the experimentally determined angles for Propellers 4661 and 4710, respectively*.

The unsteady theory of Tsakonas et al (6,7) predicts a similar trend of $\kappa_{(Fx)1}$ with J in axial and tangential wakes; i.e., the predicted $\kappa_{(Fx)1}$ tends to increase with increasing J and $\partial\kappa/\partial J$ to decrease with increasing J . These predicted trends are similar because this method considers only the component of wake resolved normal to the blade pitch line, for either longitudinal or tangential wakes. Thus, as discussed previously, this method does not distinguish between longitudinal and tangential wakes.

The trend of $\kappa_{(Fx)1}$ with J predicted by the method of Tsakonas et al does not agree with the experimental results. At low values of J ; i.e., high time-average loading coefficient, this method gives the worst correlation with experimental results among the three methods evaluated. This occurs, in part, because the theory does not account for the influence of the time-average loading. As discussed in the preceding section, it is unclear why this method predicts that the loading coefficient decreases with decreasing J , rather than predicting that it is insensitive to J .

Near design J , the method of Tsakonas et al (6,7) predicts $\kappa_{(Fx)1}$ in longitudinal wakes which is close to the predictions by the other calculation methods, and reasonably close to experimental results. In contrast, in inclined flow the method of Tsakonas et al predicts much smaller values of $\kappa_{(Fx)1}$ than either the other calculation methods or the experiments even at design J ; see Figure 9. In particular, near design J the predictions of $\kappa_{(Fx)1}$ by Tsakonas et al agree with the predictions of Kerwin and Lee in longitudinal flow but not in inclined flow. This suggests that the tangential inflow velocities significantly influence the periodic blade loads in a manner which is considered by the method of Kerwin and Lee but which is not properly considered by the method of Tsakonas et al.

*Recall that Propeller 4661 rotates left-hand and propeller 4710 rotates right-hand, and the phase angle is the angle of the blade reference line which the maximum positive loading occurs measured from the upward vertical positive in the direction of propeller rotation.

The unsteady method of Tsakonas et al predicts that the maximum value of $\kappa(F_x)_1$ in the longitudinal wake will occur at approximately 10 degrees after the experimental value for Propeller 4661 and approximately 10 degrees before the experimental value for Propeller 4710; see Figure 13.

The variations of $\kappa(F_x)_1$ predicted by the method of Kerwin and Lee (8) agrees more closely with the experimental results than either of the other two methods evaluated. However, the agreement with experimental results is not as good as that obtained in inclined flow by the method of Kerwin.

The magnitude and the variation of the phases with advance coefficient predicted by the method of Kerwin and Lee agree with the experimental results substantially better than do those predicted by either of the other two predictions evaluated. Except for $J > 1.0$ on Propeller 4710, the phases predicted by Kerwin and Lee are within 5 degrees of the experimental phases.

In summary, all three of the calculation procedures predicted $\kappa(F_x)_1$ to within 20 percent of the experimental values at design J . However, the agreement at substantially off-design J was not as good. In general, the method of Kerwin and Lee gave the best agreement with experimental results in the magnitude and trend of $\kappa(F_x)_1$ over a range of J . In addition, the method of Kerwin and Lee gave the best agreement with experimental results in phases and in the trends of the variation of phases with J .

SUMMARY AND CONCLUSIONS

An investigation was undertaken to evaluate the periodic single-blade loads on propellers and the influence of a nearby solid boundary on the periodic blade loads in inclined flow and in circumferentially non-uniform longitudinal velocity fields. Systematic model experiments were conducted and the results were correlated with predictions by the following methods:

1. A simple quasi-steady procedure developed by McCarthy at DTNSRDC which utilizes the open water characteristics of the propeller.
2. A linearized lightly-loaded unsteady lifting surface theory developed by Tsakonas and his colleagues at Davidson Laboratory.

3. A moderately-loaded unsteady lifting surface theory developed by Kerwin and Lee at MIT.
4. A refinement by Kerwin to the method of Kerwin and Lee which considers the inclination of the propeller slipstream for operation in inclined flow.

The results are as follows:

1. In inclined flow, all four of the calculation methods evaluated consistently underpredicted the experimental values of the periodic propeller blade loads. The method of Kerwin, which considers the inclination of the slipstream relative to the propeller axis, produced the best correlation with experimental values, and the method of Tsakonas et al produced the worst correlation with experimental values. The correlation of each method evaluated is as follows:

- a. The method of Tsakonas et al predicts the first harmonic loading to be approximately 35 percent of the experimental value at the lowest advance coefficient investigated, 65 percent of the experimental value at the design condition and 80 percent of the experimental value at the highest advance coefficient investigated. This method predicts a variation of first harmonic loading coefficients with advance coefficient which is substantially different from that obtained experimentally. This method predicts that the maximum values of loading will occur at approximately 15 to 20 degrees of blade angular position before the experimentally determined angle.
- b. The quasi-steady method of McCarthy underestimates the first harmonic loading by 10 to 30 percent over a range of advance of coefficients with closer agreement at higher values of J . This method predicted a similar trend to the experimental data; i.e., that the loading coefficient decreases with increasing J . This method predicts that the maximum values of loading will occur at approximately 10 to 20 degrees before the experimentally determined angle.

- c. The unsteady theory of Kerwin and Lee showed, in general, somewhat better agreement with experimental data over a range of advance coefficient than either the quasi-steady method of McCarthy or the unsteady method of Tsakonas et al. This applies to both amplitudes and phases. This method underpredicted the periodic loads by approximately 5 to 20 percent of the experimental values, with closer agreement being obtained for the F_x and M_y components at the higher values of J . This method predicts the phases to within 5 to 15 degrees of the experimental values for most, but not all, conditions evaluated. In general, the agreement is better for the higher values of advance coefficient J ; i.e., J near or higher than the design value.
- d. The method of Kerwin, which is the only method evaluated that considers the inclination of the slipstream relative to the propeller axis, produced consistently the best agreement with experimental data, including both amplitudes and phases over the range of parameters evaluated. In particular, for low values of J this method yielded substantially better correlation with experimental results than any of the other methods evaluated. At high values of advance coefficient this method yields substantially the same results as the method of Kerwin and Lee. Thus, the inclination of the propeller slipstream relative to the propeller axis can significantly influence the periodic propeller blade loads, and the importance of this inclination increases with increasing time-average loading.

2. In longitudinal flow, all of the calculation procedures evaluated predict the amplitude of the periodic single-blade axial force to within 20 percent of the experimental values at design J . However, the agreement at substantially off-design J is not as good. In general, the method of Kerwin and Lee agrees best with experimental results in the magnitude and the trend of periodic single-blade axial force coefficient over a range of J . In addition, the method of Kerwin and Lee agrees the best with experimental phases and in the trends of the variation of phases with J .

- 3. The periodic blade loads in inclined flow are not significantly influenced by the presence of a nearby boundary.

ACKNOWLEDGEMENTS

The work reported herein was funded by the Naval Sea Systems Command (NAVSEA 05R), Task ARea S)379-SL001, Task 19977.

The authors are indebted to many members of the staff of the David W. Taylor Naval Ship Research and Development Center. Special appreciation is extended to Mr. Michael Jeffers for development of the on-line data analysis system, to Mr. Benjamin Wisler for assistance in conducting experiment, to Dr. William B. Morgan and Mr. Richard A. Cumming for overall guidance.

The authors also wish to acknowledge Mr. Claude Williams of ORI, Inc., for assistance in handling propeller performance computer programs.

REFERENCES

1. Boswell, R.J., et al, "Experimental Determination of Mean and Unsteady Loads on a Model CP Propeller Blade for Various Simulated Modes of Ship Operation," The Eleventh Symposium on Naval Hydrodynamics, Sponsored Jointly by the Office of Naval Research and University College London, Mechanical Engineering Publications Limited, London and New York, pp 789-834 (Apr 1976).
2. Boswell, R.J., J.J. Nelka, and S.B. Denny, "Experimental Unsteady and Mean Loads on a CP Propeller Blade on the FF-1088 for Simulated Modes of Operation," DTNSRDC Report 76-0125, Defense Documentation Center ADA-34804 (Oct 1976).
3. Jessup, S.D., R.J. Boswell, and J.J. Nelka, "Experimental Unsteady and Time-Average Loads on the Blades of the CP Propeller on a Model of the DD-963 Class Destroyer for Simulated Modes of Operation," DTNSRDC Report 77-0110, Defense Documentation Center ADA-048385 (Dec 1977).

4. Boswell, R.J., S.D. Jessup, and J.J. Nelka, "Experimental Time-Average and Unsteady Loads on the Blades of a CP Propeller Behind a Model of the DD-963 Class Destroyer," *Propellers 78 Symposium*, The Society of Naval Architects and Marine Engineers Publication S-6, Virginia Beach, Virginia, pp 7/1-7/28 (24-25 May 1978).
5. McCarthy, J.H., "On the Calculation of Thrust and Torque Fluctuations of Propellers in Nonuniform Wake Flow," DTMB Report 1533 (Oct 1961).
6. Tsakonas, S., et al, "An Exact Linear Lifting Surface Theory for Marine Propeller in a Nonuniform Flow Field," *Journal of Ship Research*, Vol. 17, No. 4, pp 196-207 (Dec 1974).
7. Tsakonas, S. et al, "Documentation of a Computer Program for the Pressure Distribution, Forces and Moments on Ship Propellers in Hull Wakes," (In Four Volumes), Stevens Institute of Technology, Davidson Laboratory Report SIT-DL-76-1863 (January 1976) Revised April 1977.
8. Kerwin, J.E. and C.S. Lee, "Prediction of Steady and Unsteady Marine Propeller Performance by Numerical Lifting Surface Theory," *Transactions of the Society of Naval Architects and Marine Engineers*, Vol 86, pp 218-253 (1978).
9. Kerwin, J.E., "The Effect of Trailing Vortex Asymmetry on Unsteady Propeller Blade Forces," MIT Department of Ocean Engineering Report on contract N00014-77-C-0810, MIT OSP 85871 (May 1979).
10. Boswell, R.J. and S.D. Jessup, "Experimental Determination of Periodic Propeller Blade Loads in a Towing Tank," Proceeding of the 18th American Towing Tank Conference, U.S. Naval Academy, Annapolis, Maryland, Vol I, pp 263-270 (Aug 1977).
11. Santelli, N., et al, "Experimental Determination of Two Components of Field Point Velocities Around a Model Propeller in Uniform and Inclined Flow," Report DTNSRDC/SPD/0921-01 (Feb 1980).
12. Wereldsma, R., "Tendencies of Marine Propeller Shaft Excitations," *International Shipbuilding Progress*, Vol. 19, No. 218, pp. 328-332 (Oct 1972).
13. Meyne, K. and A. Nolte, "Experimentelle Untersuchungen der hydrodynamischen Kräfte und Momente an einem Flügel eines Schiffspropellers bei schräger Anstromung, (Experimental Investigations of Hydrodynamic Forces and Moments on One Blade of a Ship's Propeller with Oblique On-Flow)," *Schiff und Hafen*, Vol. 21, No. 5, pp. 359-366 (May 1969).
14. Bednarzik, R., "Untersuchung über die Belastungsschwankungen am Einzelflügel schräg angestromter Propeller, (Investigation of Fluctuating Loads on a Single Blade on Propellers in Oblique On-Flow)," *Schiffbauforschung*, Vol. 8, No. 1/2, pp. 57-80 (1969).
15. Blaurock, J., "Untersuchung über das Kavitationsverhalten und die instationäre Belastung von Schiffpropellern bei chraganstromung, (Investigation of Cavitation Behavior and Unsteady Loading of Ship's Propellers with Oblique On-Flow)," *Forschungszentrum des deutschen Schiffbaus*, Bericht 66/1976 (1976).
16. Raestad, A.E., "Hydrodynamic Propeller Loading in the Behind Condition," *Det norske Veritas Research Department Report 74 31-M* (May 1974).
17. Boswell, R.J. and M.L. Miller, "Unsteady Propeller Loading - Measurement, Correlation with Theory, and Parametric Study," NSRDC Report 2625 (Oct 1968).

18. Nelka, J.J., "Experimental Evaluation of a Series of Skewed Propellers with Forward Rake; Open-Water Performance, Cavitation Performance, Field-Point Pressures and Unsteady Propeller Loading," NSRDC Report 4113 (Jul 1974).
19. Valentine, D.T. and R.D. Kader, "Experimental Investigation of the Effect of Propeller Blade Pitch on Propeller-Produced Unsteady Bearing Forces and Moments," DTNSRDC Report 76-0137 (Dec 1976).
20. Valentine, D.T., "Linearized Unsteady Lifting Surface Theory of a Lightly Loaded Propeller in an Inclined Flow," Davidson Laboratory Report SIT-DL-79-9-2064 (Aug 1979).
21. Tsakonas, S., et al., "Unsteady Propeller Lifting Surface Theory with Finite Number of Chordwise Modes," Stevens Institute of Technology, Davidson Laboratory Report 1113 (Dec 1966).

INITIAL DISTRIBUTION

Copies		Copies	
1	ARMY CHIEF OF RES & DIV	37	NAVSEA (Continued)
1	ARMY ENGR R&D LAB		1 PMS-378
2	CHONR		1 PMS-380
	1 Code 438		1 PMS-381
	1 LIB		1 PMS-383
1	NRL		1 PMS-389
4	ONR BOSTON		1 PMS-391
4	ONR CHICAGO		1 PMS-392
4	ONR LONDON, ENGLAND		1 PMS-393
2	USNA		1 PMS-397
	1 LIB		1 PMS-399
	1 JOHNSON		1 PMS-400
1	NAVPGSCOL LIB		1 SEA Tech Rep Bath, England
1	NROTC & NAVADMINU, MIT		2 DET NORFOLK (Sec 6660)
1	NADC		1 FAC 032C
5	NOSC		1 MILITARY SEALIFT COMMAND (M-4EX)
	1 1311 LIB		1 NAVSHIPYD/PTSMH
	1 6005		1 NAVSHIPYD/PHILA
	1 13111 LIB		1 NAVSHIPYD/NORVA
	1 2501/HOYT		1 NAVSHIPYD/CHASN
	1 NELSON		1 NAVSHIPYD/LBEACH
1	NWC		1 NAVSHIPYD/MARE
37	NAVSEA		1 NAVSHIPYD/PUGET
	1 SEA 032		1 NAVSHIPYD/PEARL
	1 SEA 0321		12 DTIC
	1 SEA 03D		2 HQS COGARD
	1 SEA 052		1 US COAST GUARD (G-ENE-4A)
	3 SEA 0521		1 LC/SCI & TECH DIV
	1 SEA 0522		
	3 SEA 0524		
	1 SEA 0525		8 MARAD
	3 SEA 05D		1 DIV SHIP DES
	3 SEA 05H		1 COORD RES
	5 SEA 05R		1 SCHUBERT

Copies		Copies	
8	MARAD (Continued)	3	HARVARD U
1	FALLS	1	MCKAY LIB
1	DASHNAW	1	BIRKOFF
1	HAMMER	1	CARRIER
1	LASKY	2	U HAWAII/BRETSCHNEIDER
1	SIEBOLD		
2	MMA	1	U ILLINOIS/ROBERTSON
1	LIB	2	U IOWA
1	MARITIME RES CEN	1	IHR/KENNEDY
2	NASA STIF	1	IHR/LANDWEBER
1	DIR RES	2	JOHNS HOPKINS U
1	NSF ENGR DIV LIB	1	PHILLIPS
1	INST COOP RES	1	KANSAS CIV ENGR LIB
1	DOT LIB	1	KANSAS ST U ENGR EXP/LIB
1	U BRIDGEPORT/URAM	1	LEHIGH U FRITZ ENGR LAB LIB
2	U CAL BERKELEY/DEPT NAME	1	LONG ISLAND U
1	NAME LIB	4	ORI, INC
1	WEBSTER	2	KIM
1	U CAL SAN DIEGO/ELLIS	1	SCHNEIDER
2	UC SCRIPPS	1	WILLIAMS
1	POLLACK		
1	SILVERMAN		
1	U MARYLAND/GLEN MARTIN INST	5	MIT
4	CIT	1	BARKER ENGR LIB
1	AERO LIB	2	OCEAN ENGR/KERWIN
1	ACOSTA	1	OCEAN ENGR/LEEHEY
1	PLESSET	1	OCEAN ENGR/NEWMAN
1	WU	3	U MINNESOTA SAFHL
1	CATHOLIC U	1	KILLEEN
1	COLORADO STATE U/ALBERTSON	1	SONG
1	U CONNECTICUT/SCOTTRON	1	WETZEL
1	CORNELL U/SEARS	2	STATE U MARITIME COLL
1	FLORIDA ATLANTIC U OE LIB	S U ARL LIB	
		1	ENGR DEPT
		1	INST MATH SCI
		1	NOTRE DAME ENGR LIB

Copies		Copies
5	PENN STATE U ARL 1 LIB 1 HENDERSON 1 GEARHART 1 PARKIN 1 THOMPSON	1 WPI ALDEN HYDR LAB LIB 1 ASME/RES COMM INFO 1 ASNE 1 SNAME
1	PRINCETON U/MELLOR	1 AERO JET-GENERAL/BECKWITH
1	RENSSELAER/DEPT MATH	1 ALLIS CHALMERS, YORK, PA
1	ST JOHNS U	1 AVCO LYCOMING
3	SWRI 1 APPLIED MECH REVIEW 1 ABRAMSON 1 BURNSIDE	1 BAKER MANUFACTURING 2 BATH IRON WORKS CORP 1 HANSEN 1 FFG PROJECT OFFICE
1	BOEING ADV AMR SYS DIV	1 BETHLEHEM STEEL SPARROWS
2	BOLT BERANEK AND NEWMAN 1 BROWN 1 JACKSON	3 BIRD-JOHNSON CO 1 CASE 1 RIDLEY 1 NORTON
1	BREWER ENGR LAB	2 DOUGLAS AIRCRAFT 1 TECHNICAL LIBRARY 1 SMITH
1	CAMBRIDGE ACOUS/JUNGER	2 EXXON RES DIV 1 LIB 1 FITZGERALD
1	CALSPAN, INC/RITTER	1 FRIEDE & GOLDMAN/MICHEL
1	STANDFORD U/ASHLEY	1 GEN DYN CONVAIR ASW-MARINE SCIENCES
1	STANDFORD RES INST LIB	3 GIBBS & COX 1 TECH LIB 1 OLSON 1 CAPT NELSON
3	SIT DAVIDSON LAB 1 LIB 1 BRESLIN 1 TSIAKONAS	1 GRUMMAN AEROSPACE/CARL
1	TEXAS U ARL LIB	3 HYDRONAUTICS 1 ETTER 1 SCHERRER 1 LIBRARY
1	UTAH STATE U/JEPPSON	
2	WEBB INST 1 WARD 1 HADLER	
1	WHOI OCEAN ENGR DEPT	

Copies		Copies		
1	INGALLS SHIPBUILDING	1	TRACOR	
1	INST FOR DEFENSE ANAL	1	UA HAMILTON STANDARD/CORNELL	
1	ITEK VIDYA		CENTER DISTRIBUTION	
1	LIPS, INC	Copies	Code	Name
1	LITTLETON R & ENGR CORP/REED	1	11	Ellsworth
1	LITTON INDUSTRIES	1	1102.1	Nakonechny
1	LOCKHEED/WAID	1	15	Morgan
1	MARITECH, INC/VASSILOPOULIS	1	1509	Pollard
3	HYDRODYNAMICS RESEARCH ASSOCIATES, INC	1	152	Lin
1	COX	1	1521	Pien
1	VALENTINE	1	1528	Lee
1	NELKA	1	1528	Reed
1		1	1528	Dobay
1	NATIONAL STEEL & SHIPBLDG	1	154	McCarthy
		1	1543	Cumming
1	NEWPORT NEWS SHIPBLDG LIB	1	1544	Brockett
		30	1544	Boswell
1	NIELSEN ENGR/SPANGLER	10	1544	Jessup
1	HYDROMECHANICS, INC/KAPLIN	1	1552	Huang
		1	1556	Santore
1	NAR SPACE/UJIHARA	1	1556	Wisler
		1	1556	Jeffers
1	PROPULSION DYNAMICS, INC	1	172	Krenzke
1	PROPULSION SYSTEMS, INC	1	1720.6	Rockwell
1	SCIENCE APPLICATIONS, INC/STERN	1	19	Sevick
1	GEORGE G. SHARP	1	19	Strasberg
1	SPERRY SYS MGMT LIB/SHAPIRO	1	1903	Chertock
2	SUN SHIPBLDG	1	1962	Zaloumis
	1 LIBRARY	1	1962	Noonan
	1 NEILSON	1	2814	Czyryca
1	ROBERT TAGGART	10	5211.1	Reports Distribution
		1	522.1	Library (C)
1	TETRA TECH PASADENA/CHAPKIS	1	522.2	Library (A)

DTNSRDC ISSUES THREE TYPES OF REPORTS

1. DTNSRDC REPORTS, A FORMAL SERIES, CONTAIN INFORMATION OF PERMANENT TECHNICAL VALUE. THEY CARRY A CONSECUTIVE NUMERICAL IDENTIFICATION REGARDLESS OF THEIR CLASSIFICATION OR THE ORIGINATING DEPARTMENT.
2. DEPARTMENTAL REPORTS, A SEMIFORMAL SERIES, CONTAIN INFORMATION OF A PRELIMINARY, TEMPORARY, OR PROPRIETARY NATURE OR OF LIMITED INTEREST OR SIGNIFICANCE. THEY CARRY A DEPARTMENTAL ALPHANUMERICAL IDENTIFICATION.
3. TECHNICAL MEMORANDA, AN INFORMAL SERIES, CONTAIN TECHNICAL DOCUMENTATION OF LIMITED USE AND INTEREST. THEY ARE PRIMARILY WORKING PAPERS INTENDED FOR INTERNAL USE. THEY CARRY AN IDENTIFYING NUMBER WHICH INDICATES THEIR TYPE AND THE NUMERICAL CODE OF THE ORIGINATING DEPARTMENT. ANY DISTRIBUTION OUTSIDE DTNSRDC MUST BE APPROVED BY THE HEAD OF THE ORIGINATING DEPARTMENT ON A CASE-BY-CASE BASIS.



